AMM-In_xSi, a microporous catalyst for the oxidative dimerization of propene with air

Saule Bukeikhanova [a], Holger Orzesek [a], Uwe Kolb [a], Klaus Kühlein [b] and Wilhelm F. Maier [a,*]

[a] *Max-Planck-Institut für Kohlenforschung, Kaiser-Wilhelm-Platz 1, D-45470 Mülheim a.d. Ruhr, Germany*
[b] *HOECHST AG, D-65926 Frankfurt am Main, Germany*

Received 7 October 1997; accepted 25 November 1997

Amorphous microporous mixed oxides of indium and silicon (AMM-In_xSi) have been prepared by our acid-catalyzed sol–gel method. The materials are amorphous with a narrow pore-size distribution with pore widths around 0.7 nm, a surface area about 500–800 $m^2\ g^{-1}$ (BET) and contain homogeneously distributed In-centers in the silicon matrix (XRD, TEM, EXAFS). These materials have been found to be excellent catalysts for the oxidative dimerization of propene with air to 1,5-hexadiene with high selectivity. The best reaction conditions found are gas phase, normal pressure at 550–600°C. Propene conversion has reached 10% with selectivities > 80%.

Keywords: amorphous microporous mixed oxides, AMM, In–silica catalyst, selective oxidation with air, oxidative propene coupling, 1,5-hexadiene, heterogeneous catalyst, gas phase oxidation

1. Introduction

Oxidative dimerization of hydrocarbons is an attractive process for ecological and economical reasons (air as reagent, water as side product) for the upgrading of small hydrocarbons:

$$4R{-}H + O_2 \rightarrow 2R{-}R + 2H_2O$$

There has been intensive research on the dimerization of methane [1], but efforts to couple higher hydrocarbons are still limited [2]. It is already possible to obtain, for example, diallyl and benzene from propene, *p*-xylene from isobutene, dibenzyl and trans-stilbene from toluene. The main problem of these reactions is selectivity. With improved selectivity oxidative dimerization would be very useful for the conversion of small hydrocarbons into industrially important alkenes of higher molecular weight. Because of the availability of propene, its oxidative dimerization to 1,5-hexadiene is especially attractive:

$$4CH_3CH{=}CH_2 + O_2$$
$$\rightarrow 2H_2C{=}CH{-}CH_2{-}CH_2{-}CH{=}CH_2 + 2H_2O$$

However, the products of propene oxidation are highly dependent on the chemical nature of the catalyst used. With thallic oxide propene can be converted to propene oxide [3], with selenium dioxide, bismuth molybdate or copper on silica to acrolein [4] and with oxides of lead, cadmium, thallium [3,5], manganese [6], bismuth [7] or indium [5,8,9] at high temperatures (> 500°C) 1,5-hexadiene formation has been reported. With anionic, cationic or Ziegler catalysts [10] 1,5-hexadiene has been obtained as a by-product of the oligomerization and polymerization processes. However, the products of these conventional reactions tend to be mixtures of branched oligomers with a MW-distribution, so that the resulting yield of 1,5-hexadiene is rather low and its separation from the reaction mixture is too expensive.

The influence of acid–base properties has been studied on several catalysts [2,11]. It was found, that an increase of the acidity of the catalyst causes a decrease of the rate and selectivity for propene dehydrodimerization and aromatization products, while the yield of acrolein increases. At sites of lower acid strength dimerization is favored, indicating that the intermediates may have more radical type character.

Metal oxides of group III–V main group elements have been reported to catalyze this reaction more selectively [2,5,8,9]. In_2O_3- and TlO_2-catalysts were reported with selectivities peaking at 60–80% (including benzene) at propene conversions < 1% [2]. Because of the problems associated with the use of Tl as catalyst, In-oxide appears more attractive. In order to increase the catalyst activity mixed oxides, mainly based on bismuth oxide, have also been studied [8,7,12]. Here selectivities of 60% at conversions up to 28% have been reported. Highest selectivities to 1,5-hexadiene have been observed generally at temperatures above 450°C with large excess of propene.

The oxidative conversion of propene to benzene, acroleine and 1,5-hexadiene with In_2O_3 catalysts could be modeled with Langmuir–Hinshelwood type rate equations [8]. According to this model the rate-limiting step is hydrogen abstraction from propene to an allyl intermediate and the initial reaction is the formation of 1,5-hexadiene by the interaction of two molecules of propene and the dissociated O_2, all adsorbed on the surface.

* To whom correspondence should be addressed.

Propene, diallyl and acrolein are adsorbed competitively at the same sites, while oxygen is adsorbed at other sites. Acroleine formation is attributed to the reaction of surface allyl species with gas phase oxygen. The catalytic centers are indium ions capable of the formation of π-complexes with the olefin. It is assumed that this reaction proceeds via the formation of a surface π-allyl complex as the rate-determining step. The recombination of two allyl radicals in the postcatalytic volume of the reactor in the gas phase or on the surface of the catalyst are considered as major pathways for the formation of 1,5-hexadiene.

A new approach to possibly increase the selectivity of this reaction is to combine the active sites with the shape selectivity of a microporous material. It was hoped that atomically isolated active sites located in a shape-selective environment may favor the formation of the desired dimers and prevent the formation of oligomers for simple size exclusion reasons. A simple way to prepare microporous materials with homogeneously isolated active centers is the sol–gel process. We have shown that microporous oxides with a narrow pore size distribution can be prepared by an acid-catalyzed sol–gel process [13]. By the same process copolycondensation of Si-alkoxides with the alkoxides of the centers of active sites results in the domain free formation of microporous mixed oxide catalysts. Such catalysts show superior redox and isomerisation selectivity, as documented with Ti and V containing microporous silicas [14]. Such amorphous microporous mixed oxides with narrow pore-size distribution and homogeneous elemental distribution are abbreviated AMM-M_xSi, where x denotes the atomic percentage of the second oxide element relative to the bulk oxide of Si. The following equation summarizes the synthesis reaction of the AMM-materials prepared in this study:

AMM-In_xSi:

$$x\mathrm{In(NO_3)_3} + \mathrm{(EtO)_4Si} \rightarrow \mathrm{(In_2O_3)_{x/2}SiO_2}$$

2. Experimental part

2.1. Preparation of the catalysts

The catalysts have been prepared by a single-step acid-catalyzed sol–gel method, which permits structural control of the mixed oxides already during the preparation. As components for the sol have been used: $In(NO_3)_3$ as the active site precursor, tetraethoxysilane (TEOS) as the precursor for the silica matrix, EtOH as solvent and 8 N HCl as the acid catalyst for the sol–gel preparation. The amount of each component (dependent on the In-content of the resulting catalyst) for the AMM-In_xSi_y has been calculated by the following formula:

$$\mathrm{In(NO_3)_3 : Si(OEt)_4 : H_2O : HCl : EtOH} = x : y : 2(x+y) : 0.35(x+y) : 3(x+y)\,.$$

The sol–gel procedure was carried out at room temperature. For a homogeneous material free of domains it is essential, that the solution remains clear during the whole sol–gel process. The In-salt was dissolved in ethanol. Then tetraethoxysilane and hydrochloric acid were added slowly to the resulting stirred solution. The solution was then covered with Parafilm and stirring was continued with a magnetic stirrer until gelation occurred, usually after a few days. The solidified gels were heated in ambient atmosphere to a temperature of 250°C with a heating rate of 0.2°C/min and kept there for 5 h. It is necessary to mention, that the properties of these materials strongly depend on further procedures of drying and calcination. After the calcination the catalysts have been crushed and ground in a mill.

2.2. Catalyst characterization

EXAFS data acquisition and analysis. The EXAFS experiments were performed at the In K-edge (27 940 eV) at the beamline ROEMO II at HASYLAB, Hamburg, with a Si⟨311⟩ double-crystal monochromator (~4.4 GeV, 50–95 mA beam current). In all cases data were collected in transmission mode. The second crystal was detuned by about 35% from its maximum flux position to discard higher harmonics. Energy calibration was performed with In powder. Data were evaluated with a program package that is described in detail [15]. The curve fitting procedure was performed with amplitude and phase functions calculated with the program FEFF6 [16,17].

Physisorptions. Physisorption isotherms were obtained with Ar in liquid Ar on a Coulter Omnisorp 360 (continuous flow technique). The samples were heated up to 523 K for 48 h at 5×10^{-4} Pa prior to the measurement. Micropore size distributions were calculated from Ar-adsorption isotherms with the Horváth–Kawazoe method for microporous solids. Surface areas were calculated using the BET-equation in the low pressure region ($p/p_0 = 0.008$–0.01).

X-ray diffraction. X-ray powder diffraction (XRD) patterns were measured in the Debye–Scherrer technique on a STOE STADI 2/PL diffractometer using Cu K_α-radiation in the range of $2\theta = 10$–$80°$. The detector used was an area detector PSD 1. The temperature dependence of the patterns was examined in the temperature range from 323 to 1173 K (stepwise increase of 50 K prior to each measurement) and displayed after background correction.

2.3. Catalytic experiments

The experiments were carried out in the gas phase in

a fixed-bed reactor under isothermal continuous flow conditions. The catalyst powder (usually 50 mg) was positioned between two quartz wool plugs in the middle of a quartz-glass tube reactor (30 cm length; 4 mm inner diameter). The reactor was heated by an IR-furnace. The temperature was controlled by a thermocouple, positioned at the middle of the reactor, where it was heated to the required temperature and held under isothermal conditions. The flow-rate and composition of the reactant gas mixture of propene and air was regulated by two mass-flow controllers at the inlet of the reactor. Condensible parts of the product mixture were collected in a u-tube filled with 3 ml of methylcyclohexane at −78°C. The composition of the products was determined gaschromatographically (RTX-1 column) after each experiment. Selected samples of the product gas phase were collected and analyzed by quantitative mass spectrometry. The CO_2-content of the product gas of selected experiments was determined by a CO_2-sensor.

3. Results and discussion

The catalysts used here have been prepared by a sol–gel method. This inorganic hydrolysis–polycondensation reaction allows the preparation of highly porous mixed oxides at mild reaction conditions. Its big advantage over other methods like the hydrothermal procedures or traditional solid state syntheses is its control over chemical composition, pore size distribution and surface polarity in a one-step preparation procedure. Initial studies with a series of AMM-M_xSi materials showed, that AMM-In_xSi catalysts are unusually selective materials for the dimerization of propene. We have therefore studied this catalyst in more detail.

Table 1
Influence of In-content on surface area of the AMM-In_xSi catalysts

Catalyst	BET-surface area (m^2/g)
In_2O_3	< 10
AMM-Si	610
AMM-$In_{0.1}$Si	503
AMM-In_2Si	629
AMM-In_4Si	778
AMM-In_{10}Si	426

3.1. Structural and morphological data

The catalysts prepared in this study have been charac-

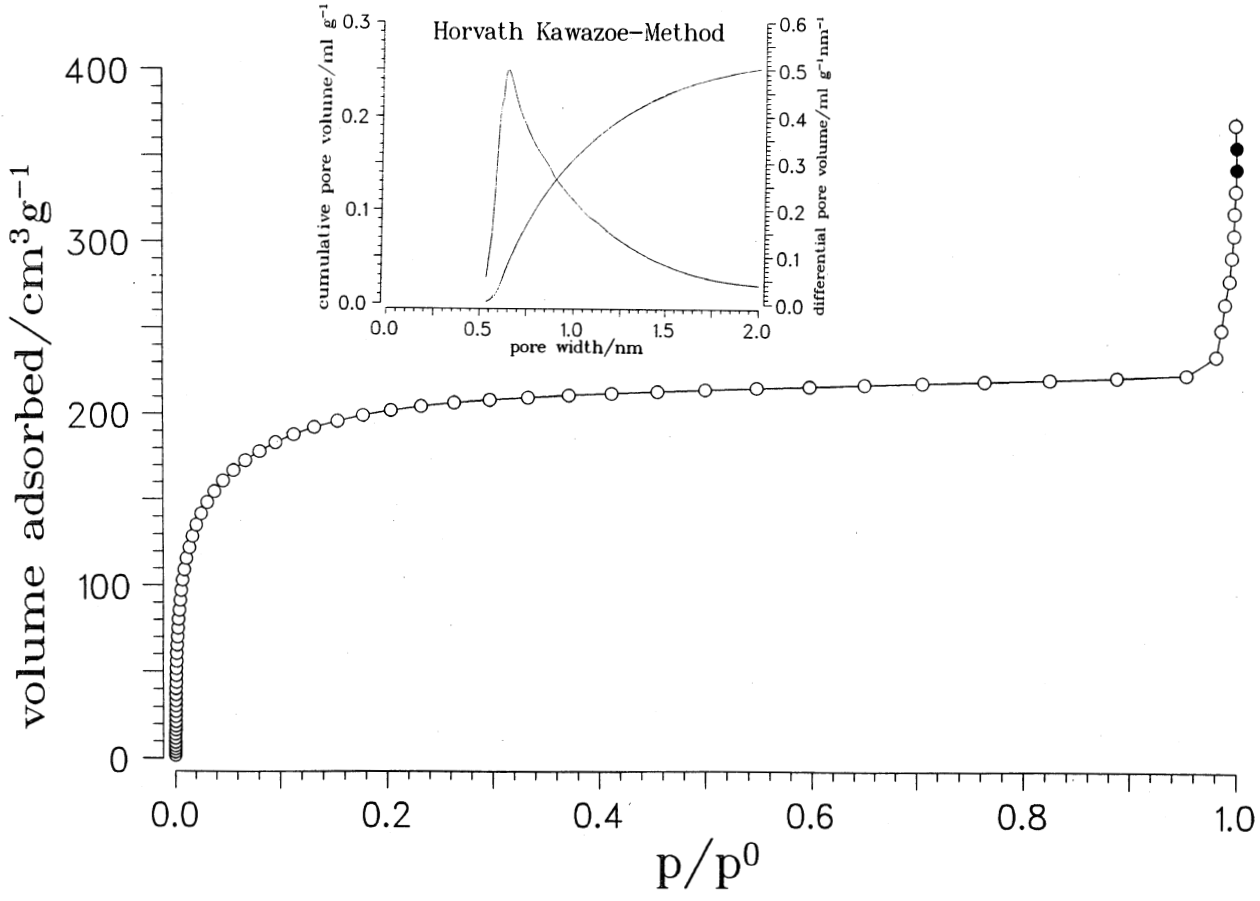

Figure 1. Ar-adsorption isotherm and pore size distribution of AMM-$In_{0.5}$Si

Table 2
Structural parameters of indium oxide (central atoms: indium) calculated from atomic positions given in ref. [19]

Back-scatterer	Distance r (Å) indium position 1	Coordination number N	Distance r (Å) indium position 2	Coordination number N
O	2.20	6	2.13/2.21/2.22	2/2/2
In	3.37	6	3.37/3.38	2/4
In	3.84	6	3.84/3.86	4/2
O	4.12	6	3.86–4.33	6
O	4.55	6	4.57/4.78/5.00	2/2/2

terized by several methods, including XRD, TEM, BET, ^{29}Si-NMR, IR, and EXAFS. All AMM-In$_x$Si materials have a significant surface area and well-developed pore structure. There is no trend of In-content affecting the surface area, as shown in table 1.

Figure 1 shows the typical adsorption isotherm of AMM-In$_x$Si indicative of micropores with a narrow pore size distribution. The pore size distribution and pore volume, determined by the Horvath–Kawazoe method [18], shows a pore diameter 0.7 nm and a porosity of about 0.3 cm^3/g.

X-ray diffraction (XRD) of the microporous silicas showed none or broad reflections typical for amorphous materials. Only the sample AMM-In$_{10}$Si showed weak but clear reflexes of In_2O_3, confirming the beginning of domain formation observed in the EXAFS studies below.

High-resolution transmission electron microscopy shows, that the AMM-In$_x$Si materials are continuous glasses, no evidence for nano-particles could be obtained. The material is amorphous even at the atomic scale confirming the XRD-results. EDX obtained from small and large selected areas indicates a homogeneous chemical composition and is evidence against the presence of significant microdomains of In- or Si-oxides.The ^{29}Si-NMR MAS (magic angle spinning) spectrum of AMM-In$_2$Si shows the presence of two types of silicon, Q^3 and Q^4, in comparable amounts (2 : 3) and much smaller amounts of Q^2 supporting a three-dimensional porous framework structure.

EXAFS data evaluation: results and discussion

Bulk indium oxide was used as reference substance. The indium atoms in indium oxide occupy two positions in the crystal structure with different local environments (see table 2)[1] . The spectrum of indium oxide was analyzed, using amplitude and phase data calculated with FEFF6 [16,17], with a standard single scattering calculation. The results are shown in table 3 and figure 2 respectively. It can be seen that the main features of the spectrum can be simulated with only three backscatterers (oxygen, indium, indium). Oxygen atoms in a longer distance can be neglected in the calculation.

To study the influence of the indium content in the AMM-In$_x$Si on the structure of the amorphous mixed oxides two different samples with $x = 2$ and $x = 10$ were investigated. In both samples a good agreement between the non-filtered and fitted $\chi(k) \cdot k^3$-function can be reached with a single scattering calculation with only two backscatterers (oxygen and chlorine, see table 4, figure 3) at short distances. The chlorine backscatterer is essential for a good agreement and the determined distance excludes that the second backscatterer is silicon, which has a similar phase function. Therefore it can be deduced that a significant amount of the indium atoms exists as indium chloride in both samples. The determined distance is in good agreement with the distance in pure indium chlorine (2.4-2.5 Å)[1]. This compound could have been formed by the hydrolysis of the indium educt with hydrochloric acid during the sol–gel preparation. No backscatterers at a longer distance are necessary for the calculations. In the Fourier transformed functions only one shell at ~2 Å can be seen (see figure 3). This indicates that the samples are amorphous. In fact, this observation is in agreement with the results of an X-ray powder diffraction analysis.

The freshly prepared AMM-In$_x$Si are amorphous and no indication for domains of indium oxide have been found. However, the catalytic reactions have been performed at 560–600°C, a temperature range in which atoms or small fragments may have enough mobility to rearrange the structure of the material. To get more information about these possible structural changes the sample AMM-In$_2$Si was analyzed also after catalysis (used catalyst) and the unused sample AMM-In$_{10}$Si was analyzed after additional calcination at 600 h for 5 h (ele-

Table 3
Results of the curve fitting procedure with FEFF6 amplitude and phase data at the In K-edge for In_2O_3. Please compare with table 2. Amplitude reducing factor S_0 was set to 1

Back-scatterer	Distance r (Å)	Coordination number N	Damping factor σ
O	2.15	5.6	0.1351
In	3.34	5.4	0.0637
In	3.83	4.8	0.0705

[1] Absorber backscatterer distances of In_2O_3 [19] and $InCl_3$ [21] were calculated on the basis of X-ray diffraction results with the program ATOMS 2.44a [20].

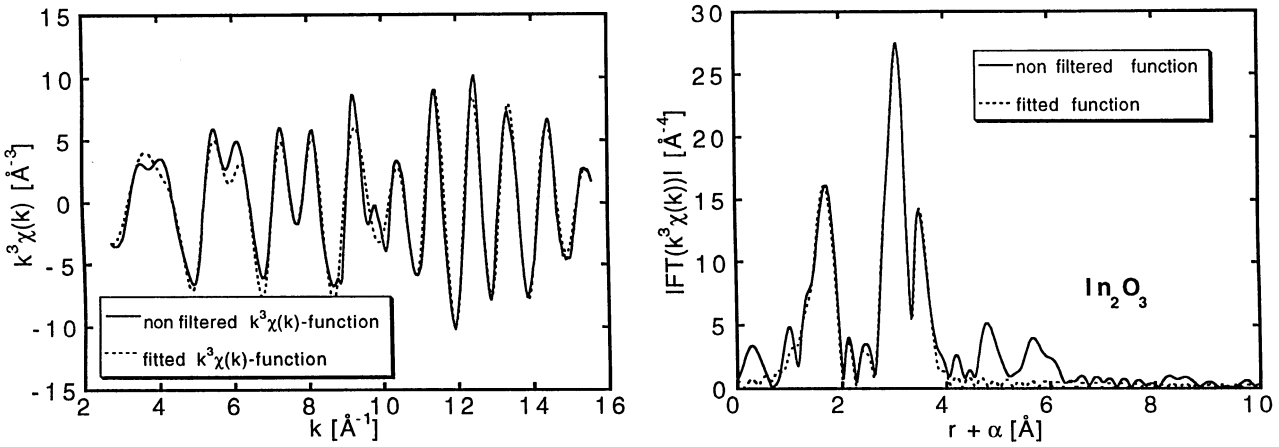

Figure 2. Non-filtered (experimental) and fitted $\chi(k) \cdot k^3$-functions and their Fourier transforms of In_2O_3.

mental analysis showed Cl at the detection limit $< 0.1\%$). The results of the curve fitting procedures are shown in table 4 and figure 3. The local environment of the sample after catalysis (figure 3) now shows a small, but distinct signal for presence of In in the second shell at 3 Å. The lack of a signal from the third or higher shells indicates, that the domains present are either very small or not completely crystalline, the low intensity of the signal at 3 Å is indicative of an atomic dispersion of the In with few domains. The local environment of the indium atoms in the calcined sample AMM-In_{10}Si, on the other hand, looks similar to the environment in indium oxide, but with smaller coordination numbers for backscatterers in longer distances. The In-oxide domains are highly crystalline and rather large. Here the lower intensities of the signals indicate either a lower crystallinity relative to bulk In-oxide (figure 2) or the simultaneous presence of atomically dispersed In in the material.

Table 4
Results of the curve fitting procedure with FEFF6 amplitude and phase data at the In K-edge. Amplitude reducing factor S_0 was set to 1

Back-scatterer	Distance r (Å)	Coordination number N	Damping factor σ
	AMM-In_2Si		
O^A	2.12	4.0	0.0965
Cl^B	2.40	2.5	0.0807
	AMM-In_{10}Si		
O^A	2.14	3.1	0.0917
Cl^B	2.42	3.2	0.0801
	AMM-In_2Si after catalysis at 560–600° C		
O^A	2.08	5.9	0.1026
In^A	3.30	1.9	0.1076
	AMM-In_{10}Si after calcination at 450° C		
O^A	2.10	6.3	0.0949
In^A	3.25	0.9	0.0402
In^A	3.91	3.1	0.0616

Therefore it can be deduced that the rearrangement of the structure leads to the formation of small indium oxide domains in the silica matrix. The chlorine backscatterer found in the freshly prepared materials is not longer necessary for the calculation of the $\chi(k) \cdot k^3$-function in both, the calcined and the used samples. Because chlorine has a greater atomic mass in comparison to oxygen its contribution to the resulting $\chi(k) \cdot k^3$-function should be large. The absence of chlorine in the calculation indicates that In–Cl components have been destroyed quantitatively by the heat treatment and that these components are not necessary for the catalysis observed.

It is very interesting how the high reaction temperature changes the structure of the catalyst. On the one hand the higher temperature in comparison to the calcination process favours the structural rearrangement of the substance. On the other hand the smaller content of indium hinders the formation of indium oxide domains. The results of the curve fitting procedure (table 4, figure 3) show that a rearrangement happens. The indium backscatterer at a distance of 3.30 Å indicates the formation of oxide domains but their crystallinity is less developed in comparison to the calcined sample. This is deduced by the absence of the indium backscatterer at ~3.9 Å, which is not necessary for the calculation. The different crystallinity of the samples can be seen clearly by comparison of the Fourier transformed $\chi(k) \cdot k^3$ functions (see figures 2 and 3).

In the starting materials the indium atoms are distributed in the silica matrix and no indium oxide domains can be detected confirming the TEM and XRD results. Under reaction conditions the formation of indium oxide domains started to appear. Their poor crystallinity is a hint that these domains are very small. In comparison the calcination of this material at lower temperature but with a higher indium content leads to more crystalline indium oxide domains, which for the AMM-In_{10}Si have also been observed with XRD.

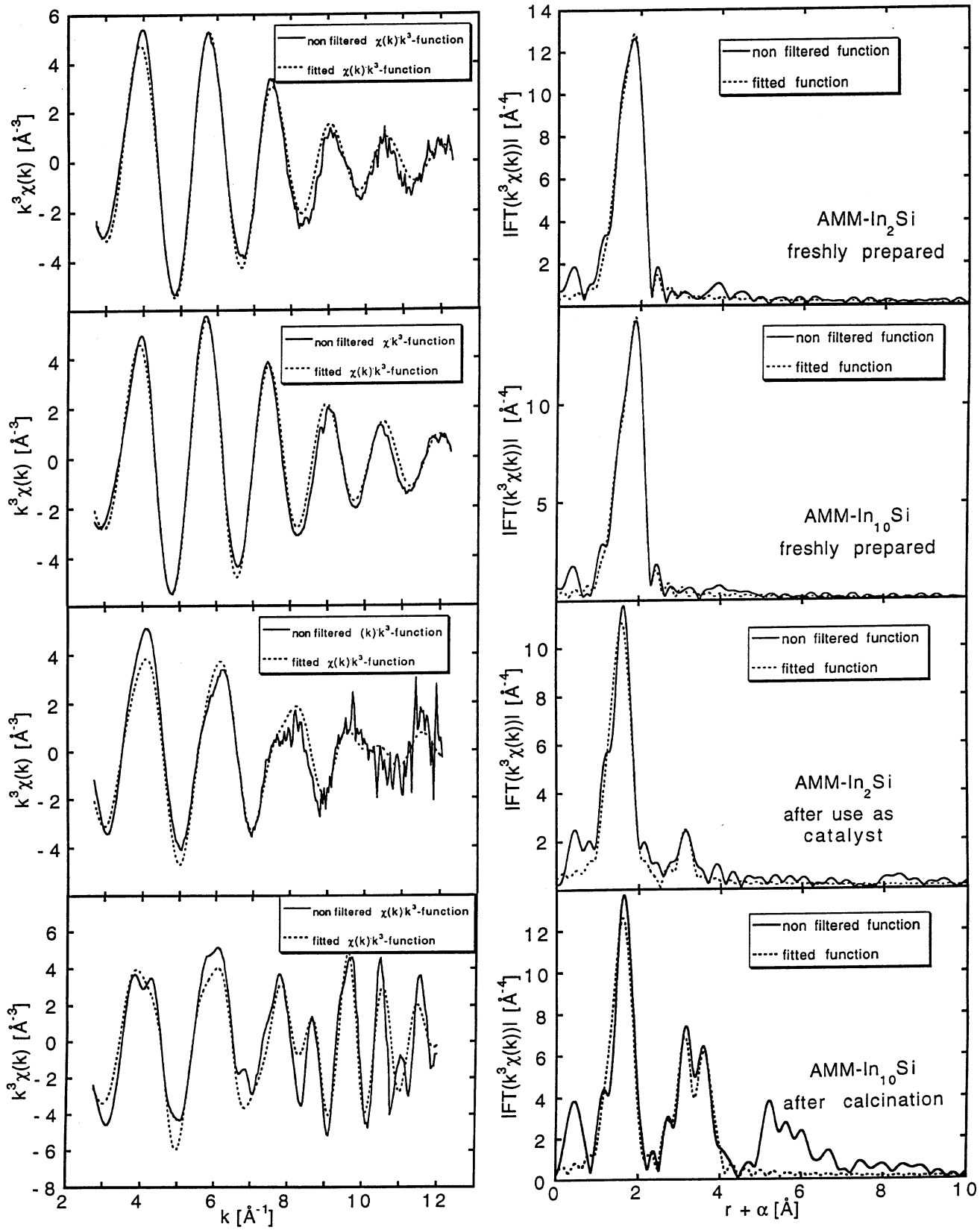

Figure 3. Non-filtered (experimental) and fitted $\chi(k) \cdot k^3$-functions and their Fourier transforms of samples AMM-In_xSi ($x = 2$, 10), AMM-In_2Si after catalysis at 560–600°C and AMM-$In_{10}Si$ after calcination at 450°C. Compare the Fourier transforms of In_2O_3 and AMM-$In_{10}Si$ after catalysis.

Table 5
Conversion and selectivity of propene to 1,5-hexadiene with various In-catalysts

Catalyst	Conversion (%)	Selectivity (%)				
		1,5-hexadiene	benzene	acroleine	1,3-butadiene	THF
In_2O_3	3	61		27		12
AMM-Si	14	61	2	23	4	10
AMM-$In_{0.1}$Si	46	80	2	7	4	7
AMM-In_2Si	59	83	1	3	4	9
AMM-In_4Si	52	79	2	6	4	9
AMM-In_{10}Si	55	80	1	7	3	9

3.2. Oxidative dimerization of propene with AMM-In_xSi catalysts

Initial experiments on the oxidation of propene with an AMM-In_2Si catalyst in the gas phase at normal pressure have shown high dimerization selectivities of > 80% to 1,5-hexadiene at propene conversions of about 10% at temperatures between 500 and 600°C. Because of the high reaction temperature, it is important to exclude autocatalysis or support effects. In table 5 the effect of the catalyst material on the reaction, studied at a large excess of propene (propene/air 19 : 1), is presented. The theoretical conversion is here limited by oxygen. AMM-Si, the microporous silica reference material, shows low activity, but it is dimerization selective with acrolein as the major by-product. Pure In_2O_3 at these reaction conditions is less active than the reference silica with a comparable selectivity. The AMM-In_xSi catalysts show independent of the In-content and despite the high conversion a rather constant high selectivity to 1,5-hexadiene. The side products may in part be attributed to the activity of the silica material. A slight trend of increasing acrolein formation with increasing In content can be seen. This points to acrolein formation on In-domains in agreement with the results from the pure In-oxide.

In a first series of experiments the influence of In-content on this dimerization reaction has been studied. Major side products are butadiene, benzene and acrolein, but also ethylene could be detected. Cyclization of 1,5-hexadiene to cyclohexene is most likely the process leading to butadiene and ethylene via a retro Diels–Alder reaction and to benzene via secondary oxidation. Examination of the product gas phase from AMM-In_2Si by mass spectrometry confirmed the presence of ethylene. The low formation of benzene is most likely the result of the low oxygen concentration. The major side product THF must form from product water and butadiene, which makes butadiene the most important side product at high conversions. CO_2-formation is negligible with the AMM-In_2Si catalyst, but increases with increasing In-content. Figure 4 summarizes the reaction network for these AMM-catalysts.

The selectivity of these catalysts to 1,5-hexadiene-formation of the AMM-In_2Si reaches 83% at an oxygen conversion of 59% and remains constant over extended reaction times of 10 h and longer. The effect of In-concentration on the catalytic performance is small. Since best results are obtained with materials with a low In-concentration, isolated In-sites are proposed as active centers.

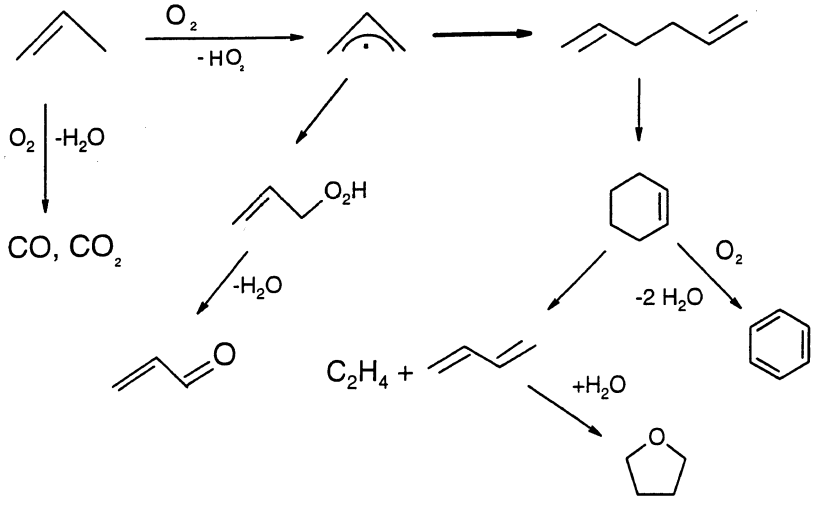

Figure 4. Reaction network of the oxidative dimerization of propene on AMM-In_xSi catalysts.

The influence of the reaction temperature on the catalytic activity and product distribution of AMM-In_2Si is shown in figure 5. There is clearly an optimal temperature range from 560 to 600°C, where 1,5-hexadiene formation is favored with a temperature around 580°C as the optimum. At temperatures below 560°C conversion drops drastically. At temperatures above 600°C secondary reactions reduce the product selectivity and increasing product decomposition leads to enhanced coke formation.

It has been observed that with these unoptimized catalysts coke formation takes place already during the initial stage of the reaction, which can be recognized by the black color of a used catalyst. After a 1 h reaction the propene/air feed was switched to Ar and the AMM-In_2Si catalyst was cooled down and removed from the reactor for surface analysis. The totally black catalyst showed no measurable surface area, even so it was still perfectly active. After air treatment of this catalyst for 3 h at 600°C complete regeneration of the original catalyst activity and selectivity was achieved, the colour turned from black to gray and the catalyst had now again a surface area of 240 m^2. Apparently, the coke has no or little effect on the catalytic properties with respect to the 1,5-hexadiene formation. The lack of surface area of the coked catalyst indicates, that the pores are filled with coke just so much as to allow effective pore diffusion at 560°C, but not at the temperatur of liquid Ar.

In another experiment oxidative dimerization of propene was continued without loss of catalytic activity for 21 h on an AMM-In_2Si catalyst at 560°C. After 8 h a slight increase of THF-formation was observed and after 16 h small amounts of unidentified oligomers could be detected. During the 21 h the 1,5-hexadiene selectivity dropped from 85 to 77%.

The bulk metal oxides mentioned above catalyze oxidation reactions during limited periods of absence of oxygen indicating oxidation activity due to available lattice oxygen. In the absence of oxygen no reaction has been observed with the AMM-In_2Si catalysts. This indicates, that the AMM-catalyst cannot utilize lattice oxygen for hydrocarbon oxidations. The reason may be the high disperions and lack of domains or the low In-concentration in these catalysts.

The role of gas-phase oxygen consists of the formation of allyl radicals: small amounts of gas-phase oxygen resulted in an increased allyl radical concentration; however, large amounts of O_2 resulted in formation of the corresponding allyl peroxy radicals.

The effect of variation of the propene–air volume ratio at 560°C is shown in figure 6. The catalyst mass and flow rate were identical for all experiments. The selectivity for 1,5-hexadiene formation increases with decreasing oxygen content of the feed, while the conversion is not affected as significantly. This confirms the general trend of this reaction discussed in the literature as mentioned above. Since conversions are calculated based on oxygen as the limiting component, the total propene conversion increases with increasing oxygen availability. The conversions and selectivities reported are based on GC-analysis of the products collected in a cold trap and the absolute conversion has been corrected by the actual oxygen conversion obtained from gas analyses. Due to experimental limitations the absolute conversion numbers may therefore carry a considerable error of several percent (table 6).

With higher oxygen content the total propene conversion increases, but also the formation of CO_2 (> 5% in the gas phase), which is indicative of undesired combustion. Benzene formation as well as acrolein formation

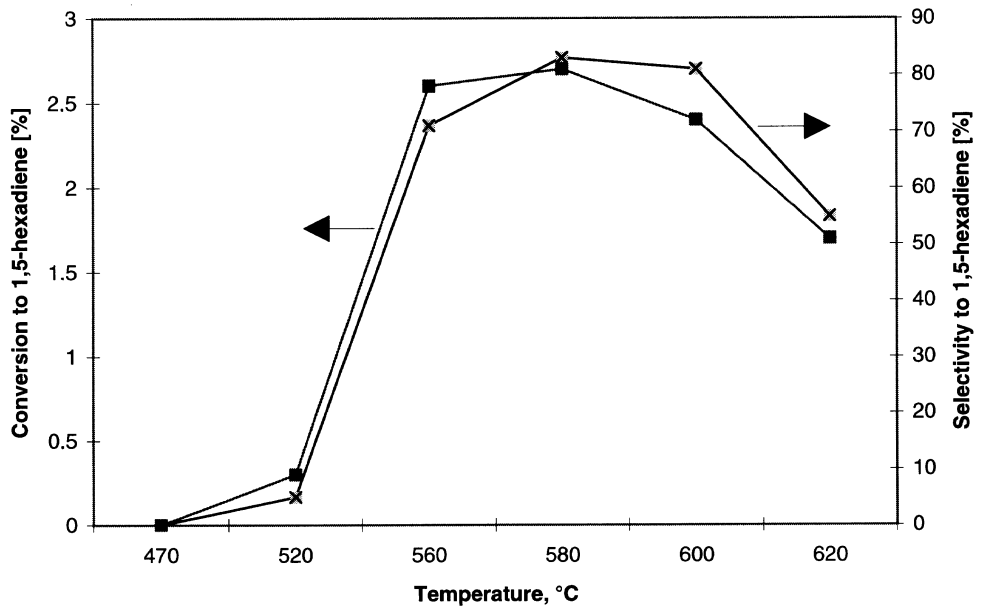

Figure 5. Effect of reaction temperature on catalytic activity and selectivity with AMM-In_2Si.

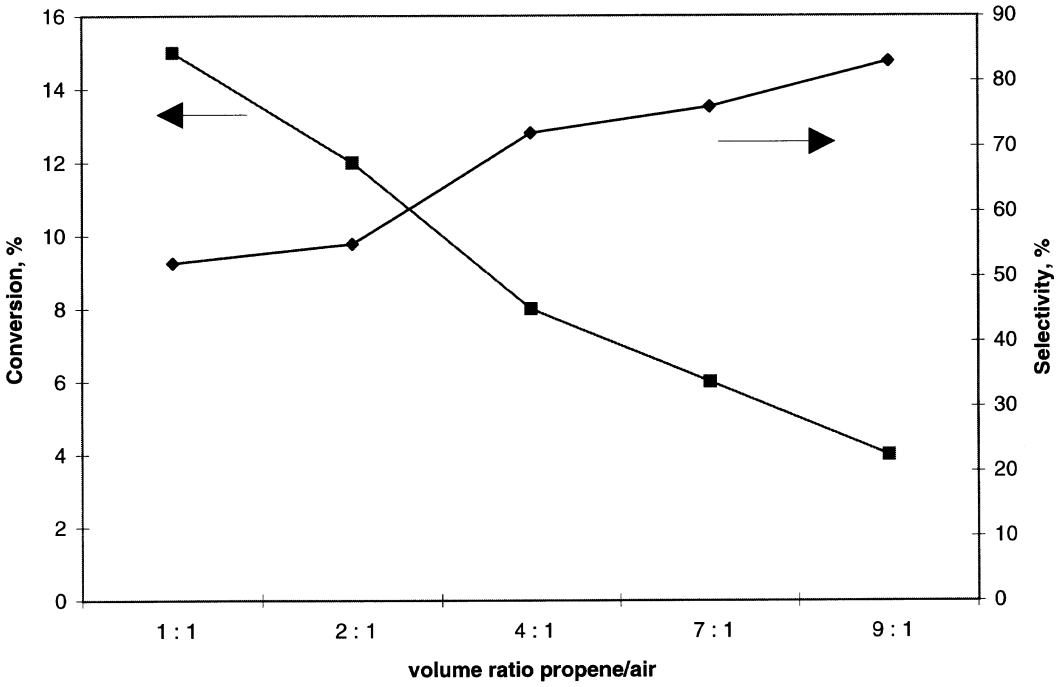

Figure 6. Effect of air concentration on activity and selectivity of 1,5-hexadiene formation.

also increase, a clear indication of their nature as secondary reactions. THF-formation decreases at the same time, which may point to THF-formation as a competition process to oxidation. Clearly, THF-formation is not limited by water availability, since water formation must increase with increasing conversion.

There is often a slight induction period at the beginning of the experiment, as shown in table 7 with the AMM-In_2Si. It takes around 40 min until the catalyst has reached a rather stable high activity. EXAFS has shown, that In is highly dispersed in the fresh catalyst samples with no indication of domains. The presence of In–Cl bonds was also noticed in the fresh samples, but not in the used samples. This documents, that the chlorine is an artefact of the preparation, not related to the desired catalysis. The induction period or change in catalytic activity of the catalyst at the beginning of the experiments shown in table 7 may be explained by the elimination of the chlorine residues, but also by a buildup of small In-oxide domains. The formation of small domains has been detected by EXAFS in the used catalyst samples AMM-In_2Si and AMM-$In_{10}Si$. The lack of good catalytic activity and selectivity of the pure In_2O_3 at our reaction conditions (table 5) shows, that large In-oxide domains are unfavorable. Since the catalytic performance of the AMM-$In_{10}Si$, where small In-oxide domain formation is more pronounced, is clearly inferior to the AMM-In_2Si material (table 5), isolated In-sites are most likely the best catalytic sites for selective dimerization of propene. However, based on the data available, small In-oxide domains as best catalytic sites cannot be excluded.

To decrease external diffusion between the gas phase and the surface of the grains, the relative velocity of the gas stream can be increased. Variation of the feed flow rate with the AMM-In_2Si catalyst (all other conditions

Table 6
Effect of feed composition on activity and selectivity of propene dimerization

Volume ratio	Conversion [a] O_2/propene (%)	Selectivity				
		1,5-hexadiene	benzene	THF	butadiene	acrolein
1 : 1	22/18	52	26	2	7	13
2 : 1	34/14	55	26	2	6	14
4 : 1	35/07	72	16	2	17	3
7 : 1	43/05	76	7	9	6	2
9 : 1	35/03	83	1	10	4	2
19 : 1	59/02.5	83	1	9	4	3

[a] Conversion is calculated from the liquid product distribution obtained by GC and the total oxygen conversion in the gas phase obtained by calibrated MS-gas analysis. Examination of the gas phase has shown, that at feed ratios $< 9 : 1$ the CO_2-formation (total combustion) cannot be neglected. Reaction conditions: AMM-In_2Si, 560°C, flow rate 86 ml/min.

Table 7
The influence of flow rate on conversion and selectivity of propylene to 1,5-hexadiene (AMM-In_2Si, reaction conditions: $T = 560°C$, propene/air 9/1)

Flow rate (ml/min)	t [a] (min)	Conversion (%)	Selectivity (%)
42	20	4	49
42	40	6	79
42	60	7	73
86	20	19	82
86	40	23	84
86	60	26	81

[a] Time after start of reaction.

kept identical) has shown a significant increase of the catalytic activity with increasing gas velocity pointing to mass transport limitations. One of the frequently used criteria for transport limitations in fixed-bed reactors, negligible external gradients, is based on the assumption that the reaction rate should be constant at constant residence time [22]. In figure 7 the effect of flow rate at constant residence is presented. Clearly, at flow rates of < 80 ml/h the reaction is diffusion limited at the external surface.

To test the importance of pore diffusion on activity and selectivity, the reaction was studied with the AMM-In_2Si of different particle sizes. Figure 8 shows a picture of the particle sizes used, obtained with the light microscope. A high total flow rate of 90 ml/min was applied to avoid external diffusion limitations. The propene/air ratio was kept at 9 : 1. Figure 9 shows the effect of particle size on the propene conversion and selectivity. Clearly, with increasing particle size the conversion drops significantly documenting pore diffusion limitations, while there is only a marginal decrease in selectivity. Product composition remains rather constant, only a slight increase in acrolein formation and a doubling of THF formation (from 6 to 10%) could be noted. This change at particle sizes below 20 μm indicates, that at these reaction conditions the reaction proceeds without significant mass transport limitations.

To test, whether this high dimerization selectivity is a general feature of In-catalysts, the dimerization of isobutene and 1-butene was examined with the AMM-In_2Si catalyst. While 1-butene conversion resulted in a mixture of dimers, isobutene was converted to 2,5-dimethyl-1,5-hexadiene with a selectivity of about 70% at a conversion of 10% at 630°C. As can be seen in table 8, a higher reaction temperature is necessary for the isobutene coupling relative to the propene coupling and the overall conversion is significantly lower. Nevertheless, the data show that the selective coupling behaviour of isolated In-sites may be a general feature applicable also to other hydrocarbons.

4. Conclusion

It was shown, that amorphous microporous mixed oxides of In and Si, prepared by a single-step sol–gel pro-

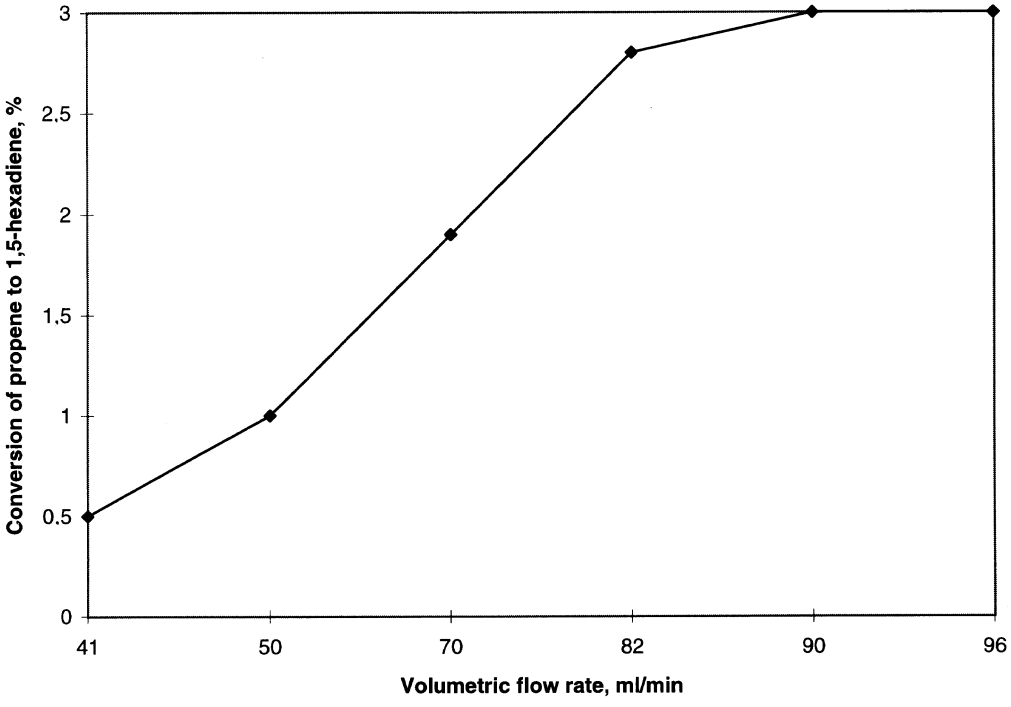

Figure 7. Effect of flow rate at constant W/F on acitivity and selectivity of 1,5-hexadiene formation.

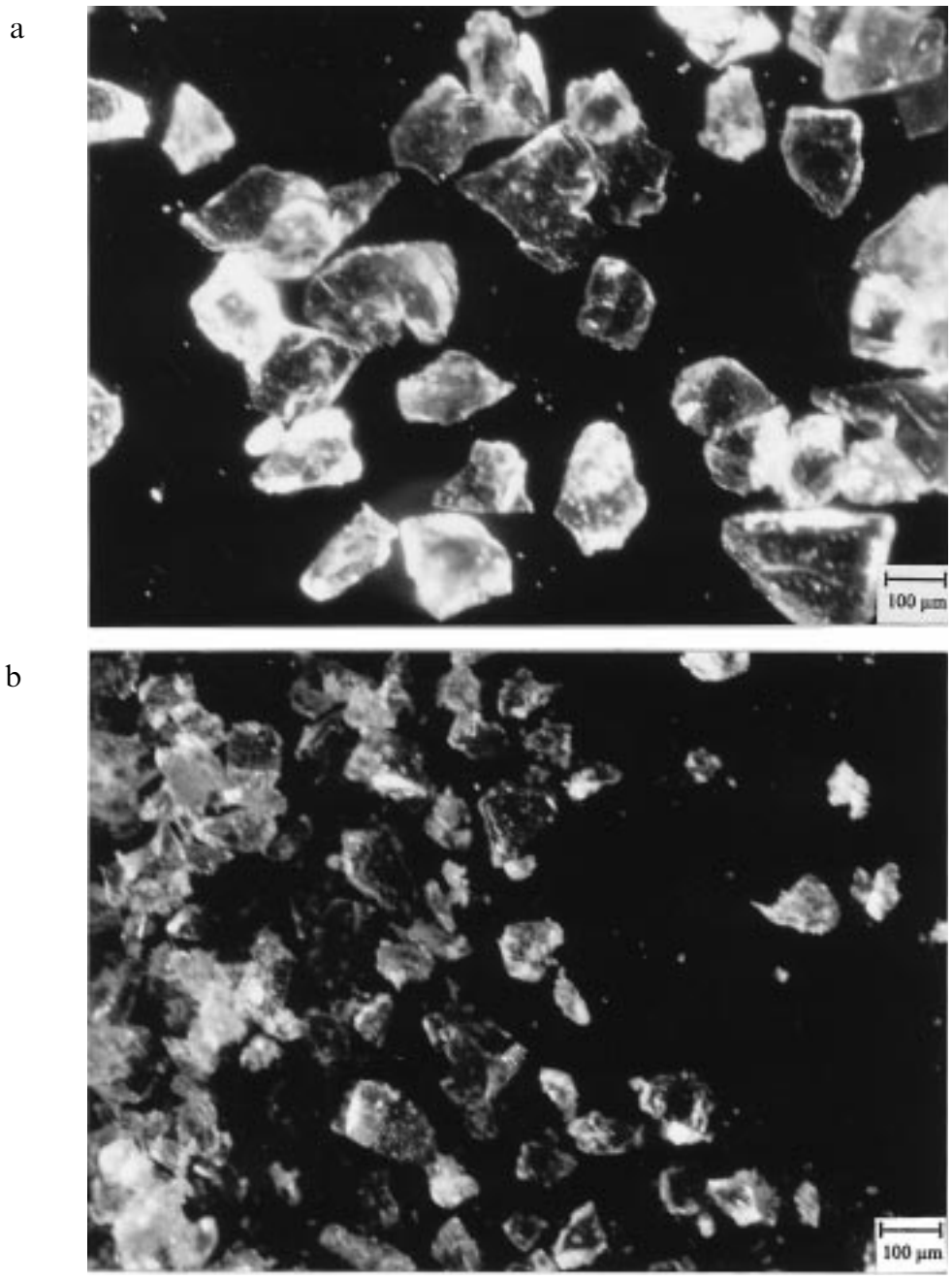

Figure 8. Light microscope pictures of particle size distributions (sieve fractions) of the AMM-In_2Si catalyst used for the studies of particle size dependence of the catalytic reaction. (a) 0.1–0.2 μm; (b) 0.02–0.05 μm; (c) finely milled powder as used in the standard experiments.

cedure, are highly selective catalysts for the oxidative coupling of olefins. This is the first time, that such a coupling reaction could be catalyzed with high selectivity. The catalysts have been characterized by a variety of analytical methods including adsorption of Ar and EXAFS. The high selectivity is attributed to the presence of isolated In-sites in the shape selective environment of the micropores of these materials, although catalytic selectivity of very small domains of In-oxide cannot be excluded. The reaction is accompanied mainly by acrolein and butadiene formation, both of which can in part be attributed to the dominating silica component of the catalyst. These side products are most likely formed at the weakly acidic surface hydroxyl groups of the silica. Deactivation of these surface hydroxyl groups of the catalyst may provide a further increase in selectivity. The study has shown, that the search for new catalytically active materials is an important one. It also shows, that the concept of isolating active centers in the shape selective environment of amorphous glasses is a promising approach opening access to a variety of new catalytic materials.

c

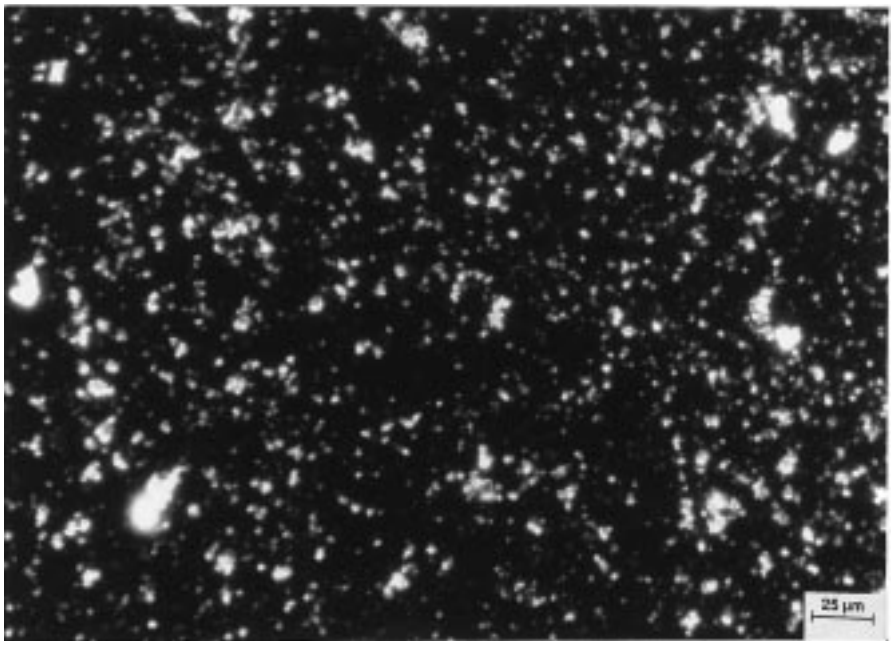

Figure 8. Continued.

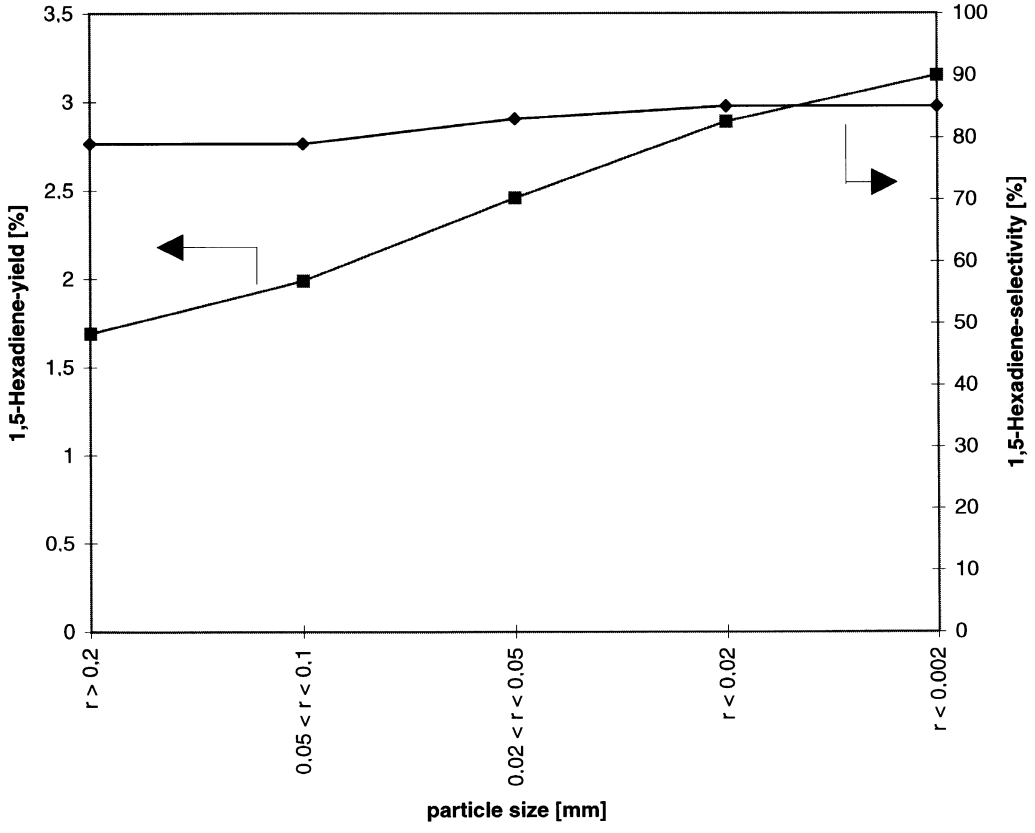

Figure 9. Effect of catalyst particle size on conversion and selectivity of propene dimerization.

Table 8
Effect of temperature on the conversion of the oxidative dimerization of isobutene with air to 2,5-dimethyl-1,5-hexadiene in the gas phase with AMM-In_2Si

	Temperature (°C)							
	570	590	600	610	630	650	670	690
O_2-conversion [a] (%)	2	4	5	5	10	11	11	11
selectivity (%)	63	70	68	62	68	62	39	30

[a] Conversion is calculated from the liquid product distribution only. Examination of the gas phase has already shown, that at feed ratios $\geqslant 9:1$ the CO_2-formation can be neglected. Reaction conditions: 50 mg AMM-In_2Si; total flow rate: 30 ml/min; butene/$O_2 = 9/2$.

Acknowledgement

SB thanks the DAAD for a fellowship and WFM the HOECHST AG for support. We thank H. Bretinger for Ar-adsorption analyses and S. Storck for HRTEM investigations.

References

[1] J.C. Mackie, Catal. Rev. Sci. Eng. 33 (1991) 169.
[2] E.A. Mamedov, Russ. Chem. Rev. 50 (1981) 291.
[3] F.N. Hill and J.P. Henry, US Patent 3,436,409 (1969).
[4] N. Kominami et al., Kogyo Kogoko Zassk. 65 (1962).
[5] D.L. Trimm and L.A. Doerr, Chem. Commun. (1970) 1303.
[6] P.A. Green, E.J. Buylos and D.E. Scheirer, Canadian Patent 788,475 (1968);
W.P. Moore Jr. and J.W. Mosier, US Patent 3,345,089 (1969).
[7] H.E. Swift, J.E. Bozik and J.A. Ondrey, J. Catal. 21 (1971) 212.
[8] J. Hagen, *Technische Katalyse* (VCH, Weinheim, 1996) pp. 337–339.
[9] D.L. Trimm and L.A. Doerr, J. Catal. 26 (1972) 1.
[10] H.M. Bank and K.H. Hayes II, European Patent EP 0 729 931 A1.
[11] D. Vanhove and B. Subagio, J. Chem. Res. Synop. 5 (1980) 176.
[12] F.E. Massoth and D.A. Scarpiello, J. Catal. 21 (1971) 225.
[13] W.F. Maier, I.C. Tilgner, M. Wiedorn and H.-C. Ko, Adv. Mat. 10 (1993) 726.
[14] W.F. Maier, S. Klein, J. Martens, J. Heilmann, R. Parton, K. Vercuysse and P.A. Jacobs, Angew. Chem. Int. Ed. 35 (1996) 180;
S. Klein, S. Thorimbert and W.F. Maier, J. Catal. 163 (1996) 477.
[15] T.S. Ertel, H. Bertagnolli, S. Hückmann, U. Kolb and D. Peter, Appl. Spectrosc. 46 (1992) 690.
[16] J. Mustre de Leon, J.J. Rehr, S.I. Zabinsky and R.C. Albers, Phys. Rev. B 44 (1991) 4146.
[17] J.J. Rehr, J. Mustre de Leon, S.I. Zabinsky and R.C. Albers, J. Am. Chem. Soc. 113 (1991) 5135.
[18] G. Horvath and K. Kawazoe, J. Chem. Eng. Jpn. 16 (1983) 470.
[19] M. Marezio, Acta Cryst. 20 (1966) 723.
[20] B. Ravel, program ATOMS 2.44a, University of Washington.
[21] D.H. Templeton and G.J. Carter, Phys. Chem. 58 (1954) 940.
[22] M. Boudart and G. Djega-Mariadassou, *Kinetics of Heterogeneous Catalytic Reactions* (Princeton University Press, Princeton, 1984).